JACS
JOURNAL OF THE AMERICAN CHEMICAL SOCIETY

COMMUNICATION

pubs.acs.org/JACS

2,5-Bis(2-octyldodecyl)pyrrolo[3,4-*c*]pyrrole-1,4-(2*H*,5*H*)-dione-Based Donor−Acceptor Alternating Copolymer Bearing 5,5′-Di(thiophen-2-yl)-2,2′-biselenophene Exhibiting 1.5 $cm^2 \cdot V^{-1} \cdot s^{-1}$ Hole Mobility in Thin-Film Transistors

Jae Seung Ha, Kyung Hwan Kim, and Dong Hoon Choi*

Department of Chemistry, Research Institute for Natural Sciences, Korea University, 5 Anam-dong, Sungbuk-gu, Seoul 136-701, Korea

Supporting Information

ABSTRACT: A novel diketopyrrolopyrrole-based π-conjugated copolymer P(DPP-*alt*-DTBSe), **5**, and a known copolymer P(DPP-*alt*-QT), **4**, have been synthesized in 80−90% yield using the Stille coupling reaction. The molecular weights of **4** and **5** are 58 781 and 19 271 g/mol, respectively, with polydispersity values of 3.25−3.35. A relatively small band gap of 1.32−1.39 eV and excellent solubility in organic solvents were achieved in the two polymers. Thin-film transistors made of **5** exhibit outstanding performance (e.g., $\mu > 1.0-1.5$ $cm^2 \cdot V^{-1} \cdot s^{-1}$, $I_{on}/I_{off} > 10^5-10^6$) with a conventional *n*-octyltrichlorosilane−SiO_2 gate dielectric.

Recent developments of p-type organic semiconductors, namely, derivatives of polyacenes, rubrene, or fused thiophene, have led to very high hole mobilities on the order of 1 $cm^2 \cdot V^{-1} \cdot s^{-1}$ in organic thin-film transistors (OTFTs).[1−5] Deposition methods for thin films of these molecules under vacuum or inert atmosphere, however, suffer from severe limitations in the large-scale fabrication of the devices owing to the complexity of the process. Unlike the small molecules mentioned above, highly conjugated semicrystalline or liquid crystalline polymers with good solution processability and film-forming abilities have been suggested as the best candidates for large-scale device fabrication owing to their potentially superior mechanical and semiconducting properties.[6−8] Thus far, *homogeneous* polymers composed of donor and acceptor units in the repeating group have been reported to have an excellent mobility of 0.94−3.3 $cm^2 \cdot V^{-1} \cdot s^{-1}$,[9] whereas specific polymer blend systems have been reported to show mobilities higher than 1.0−2.0 $cm^2 \cdot V^{-1} \cdot s^{-1}$.[10,11] However, the high crystallinity and mobility of conjugated polymers always require high molecular weight, which sometimes hampers the solubility in solvents. Moreover, the reproduction of films with identical degrees of crystallinity and molecular order remains extremely challenging, although some progress has been made using various annealing processes.[12−15] In short, the technological thrust seems to lie in the development of a new class of polymers that exhibit much better performance in practical device applications.

In this Communication, the facile synthesis of diketopyrrolopyrrole (DPP)-based conjugated polymers P(DPP-*alt*-QT), **4**, and P(DPP-*alt*-DTBSe), **5**, is demonstrated. Interestingly, the field effect mobility of **5**-based TFTs reached 1.5 $cm^2 \cdot V^{-1} \cdot s^{-1}$ after the film was annealed at 180 °C, although the molecular weight (M_n) is relatively small. TFTs made from **4** after thermal annealing at 150 °C also produce carrier mobilities of around 1.0 $cm^2 \cdot V^{-1} \cdot s^{-1}$. The best mobility of **5** is slightly higher than that of **4**. To the best of the authors' knowledge, selenophene-containing P(DPP-*alt*-DTBSe) is another promising candidate capable of showing very high mobility values, in addition to DPP-thiophene-based polymers.[9c−e]

DPP-based chromophores are often employed as high-performance organic pigments,[16] and their solubility can be improved by modifying their chemical structure.[17−19] The DPP moiety exhibits a planar conjugated bicyclic structure, which leads to strong $\pi-\pi$ interactions. DPP-containing polymers are considered promising materials for optimizing the performance of organic semiconductors.[20−22]

The polymer synthesized herein contains the DPP unit and quaterthiophene (QT) or 5,5′-di(thiophen-2-yl)-2,2′-biselenophene (DTBSe) in repeating groups. The influence of the selenium atom on the electron distribution and, therefore, on the charge transport property has been studied recently.[23−25] Since selenium generally shows a stronger heteroaromatic interaction than sulfur, the replacement of sulfur by selenium offers the opportunity to enhance the chain interaction between neighboring chains and the carrier transport phenomenon. The branched, long alkyl chains are tethered to the *N*,*N*-positions of the lactam rings to control the $\pi-\pi$ stacking and physical properties, including solubility, crystallization, energy levels, band gaps, and self-assembly capacity.

The preparation of 3,6-bis(5-bromothiophen-2-yl)-2,5-bis(2-octyldodecyl)pyrrolo[3,4-*c*]pyrrole-1,4(2*H*,5*H*)-dione, **1**, 5,5′-bis(trimethylstannyl)-2,2′-bithiophene, **2**, and 5,5′-bis(trimethylstannyl)-2,2′-biselenophene, **3**, is outlined in Scheme S1. **2** and **3** were also synthesized in a pure form by literature methods.[25−27] The synthetic procedures and characterization data are well described in the Supporting Information. Polymerization via Stille coupling was carried out using monomers **1** and **2** or **3** in the presence of tetrakis(triphenylphosphine)palladium(0) (see Scheme 1). The polymerization reaction yielded the desired polymers as dark purple solids. The resultant polymers **4** and **5** are alternating

Received: April 20, 2011
Published: June 17, 2011

Scheme 1. Polymerization of DPP-Containing Conjugated Polymers P(DPP-*alt*-QT), 4, and P(DPP-*alt*-DTBSe), 5, Exhibiting a Hole Mobility Higher than 1.0 $cm^2 \cdot V^{-1} \cdot s^{-1}$

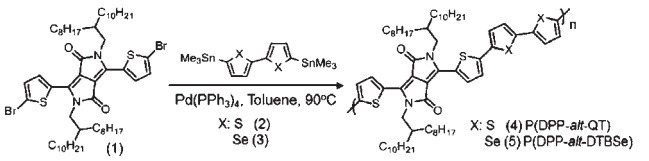

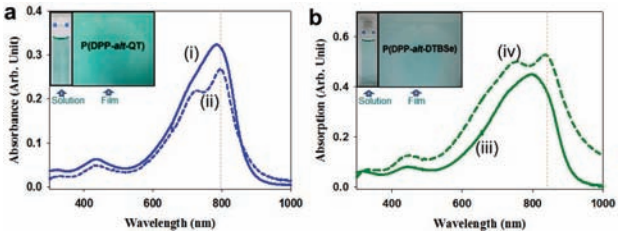

Figure 1. (a) UV−vis absorption spectra of P(DPP-*alt*-QT), **4**: (i) solution and (ii) film. (b) UV−vis absorption spectra of P(DPP-*alt*-DTBSe), **5**: (iii) solution and (iv) film. Inset: images of polymer solution and high-quality spin-coated film.

copolymers consisting of DPP and QT or DTBSe units, respectively. All of the small molecules were purified by flash column chromatography or recrystallization and were characterized by ^{1}H NMR, mass spectroscopy, and CHN elemental analysis.

The final polymers were purified by reprecipitation and Soxhlet extraction with methanol, acetone, hexane, and chloroform. They show good solubility in common solvents such as chloroform, dichloromethane, toluene, THF, and chlorobenzene (up to 12 mg/mL). New conjugated polymers having 2-(octyldodecyl) aliphatic side-chain groups are known to have a moderately high molecular weight (M_n). The M_n (19 271 g/mol) of **5** was one-third that of **4** (58 781 g/mol), with polydispersity values of 3.25−3.35. Because of the good solubility of both polymers, all measurements were done in chloroform at 35 °C.

Figure 1 shows the UV−vis absorption spectra of the polymer samples both in solution and in films. The solution spectra of both polymers are structureless. **4** exhibited absorption maxima at 784 (715 as a shoulder) nm and 796 (732) nm in the solution and film, respectively (Figure 1a). The solution spectrum of **4** showed a broad, bathochromic absorbance, which extends from 500 to 900 nm; it is attributed to the $\pi-\pi$ transition as well as the donor−acceptor (D−A) interaction between the thiophenes and DPP moieties. Two absorption bands were observed in the film samples of both polymers. In particular, the polymers in this study contain plain QT and DTBSe without any side chain, which are different from many D−A copolymers in the literature.[28−30] It can be inferred that the $\pi-\pi$ stacking of the DPP units is suppressed and the D−A interactions become more predominant. Obviously, spectrum (iv) shows a bathochromic shift by 35 nm relative to (ii), and the baseline floats significantly due to optical loss. This implies that selenophene-containing repeating groups are highly interactive, forming self-assembled molecular domains through strong electronic coupling. The optical band gaps of **4** and **5** were determined from the UV−vis absorption onsets in the solid state to be 1.39 and 1.32 eV, respectively. **5** has a much lower band gap because of its long-range effective conjugation

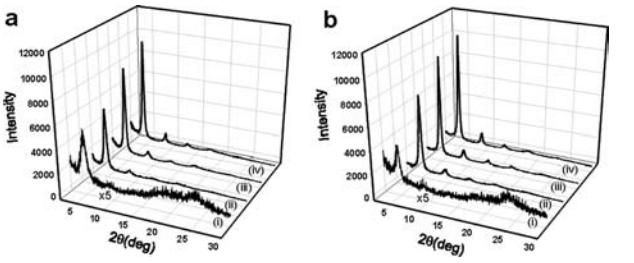

Figure 2. (a) X-ray diffraction (XRD) patterns of **4**: powder (i), as-spun film (ii), and annealed film at 100 °C (iii) and 150 °C (iv). (b) XRD patterns of **5**: powder (i), as-spun film (ii), and annealed film at 150 °C (iii) and 180 °C (iv).

length and the electron-rich nature of the selenium atom. In general, the small band gap results from the extended π-conjugation and the intra- and intermolecular interaction between donor (QT or DTBSe) and acceptor (DPP).

From the XRD patterns presented in Figure 2a, the crystalline nature of **4** is evident, and the variation of the diffraction behavior indicates the formation of well-grown polycrystallites in the spin-coated film on *n*-octyltrichlorosilane (OTS)-modified SiO_2/Si substrate. The high crystallinity of the as-spun film of **4** is attributed to the probable self-assembly into a highly ordered lamellar structure in the film. As shown in the diffractogram of the as-spun film (Figure 2a, (ii)), there are clear diffraction peaks arising from the interlayer spacing up to the fourth order. Four highly resolved diffraction peaks were observed at 2θ = 4.68° ($d_{(100)}$ =18.90 Å), 9.08°, 13.58°, and 18.08°, which indicates that the polymer chains exhibit well-organized intermolecular ordering, resulting in the enhanced crystallinity (see Figure 7S). Annealing the film at 100 and 150 °C increases the intensity of the diffraction peaks, thus indicating an increase in the crystallinity of the sample. Based on literature reports,[9] **4** forms a lamellar crystalline structure in the thermally annealed film at 150 °C, with an interlayer distance of $d_{(100)}$ = 19.10 Å and $\pi-\pi$ plane stacking distance of $d_{(010)}$ = 3.66 Å. The short interlayer distance observed implies the existence of interchain interactions induced by both $\pi-\pi$ stacking via planar molecular units and the D−A polar interaction. As for **5**, a more significantly crystalline behavior could be observed in the film sample. Before annealing the sample, we could observe relatively higher intensity of (100) diffraction peak, well-resolved fourth-order diffraction peaks, and an increase in the diffraction intensity with the annealing temperature. The diffraction peaks were clearly observed at 2θ = 4.77° ($d_{(100)}$ = 18.53 Å), 9.35°, 13.85°, and 18.34°, which revealed that the polymer chains formed a lamellar crystalline structure in the thin film. The very low intensity peak at 23.87° originating from the $\pi-\pi$−stacking distance could be barely observed. Selenophene-containing **5** also forms a lamellar crystalline structure in the film, with an interlamellar distance of ~18.53 Å (see Figure 7S). This interaction is also quite promising in terms of facilitating charge transport behavior in the TFT devices, resulting in an enhancement of the carrier mobility. The above XRD results unambiguously revealed the formation of highly ordered lamellar stacking with a presumably edge-on orientation for the annealed and even the nonannealed polymer thin films. The highly organized polymer chains in the thin films are particularly favorable for charge carrier transport via hopping through $\pi-\pi$ stacks in an OTFT device.

Because **4** and **5** exhibit high solubility in organic solvents, their thin films could easily be fabricated on an OTS-treated SiO_2

dx.doi.org/10.1021/ja203189h |*J. Am. Chem. Soc.* 2011, 133, 10364–10367

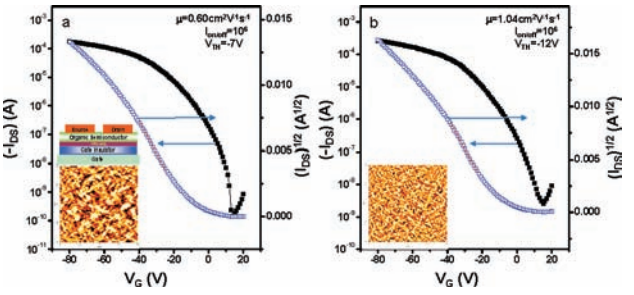

Figure 3. I_{DS} and $I_{DS}^{1/2}$ versus gate voltage (V_G) for **4**-based TFTs: (a) with the pristine film and (b) with the annealed film ($T_{ann.}$= 150 °C for 10 min). Inset: TFT device configuration and AFM images of each film sample. The performances were measured at ambient conditions.

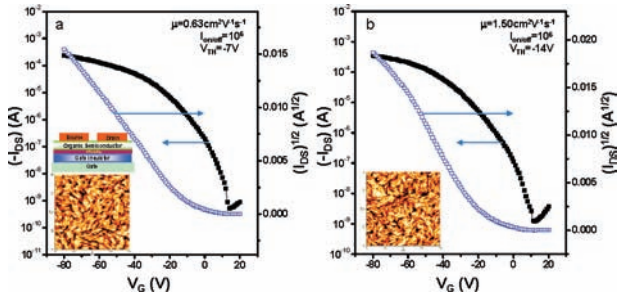

Figure 4. I_{DS} and $I_{DS}^{1/2}$ versus gate voltage (V_G) for **5**-based TFTs: (a) with the pristine film and (b) with the annealed film ($T_{ann.}$ = 180 °C for 10 min). Inset: TFT device configuration and AFM images of each film sample. The performances were measured at ambient conditions.

surface by a simple spin-coating method using a 1.0 wt % chloroform or chlorobenzene solution. Top-contact bottom gate TFT devices (W = 1500 μm, L = 100 μm) were fabricated using the polymers, and the mobilities were obtained from the source-drain current−gate voltage curves (I_{DS} vs V_G) of more than 20 devices in well-resolved saturation regions. All devices made of **4** and **5** films exhibited typical p-channel transistor behavior.

Initially, the hole mobility of the pristine film of **4** (Figure 3a) was measured to be 0.60 $cm^2 \cdot V^{-1} \cdot s^{-1}$ ($I_{on}/I_{off} \approx 10^6$, V_{th} = −7 V). However, subsequent to annealing at 150 °C, the mobility values increased to 1.04 $cm^2 \cdot V^{-1} \cdot s^{-1}$, maintaining an on−off current ratio of 10^5−10^6 (Figure 3b). The AFM images presented in the inset of Figure 3 illustrate that, after annealing at 150 °C, the polymer film surface was filled with uniform intertwined polymer fibers that afford densely interconnected chain networks.

The devices made of **5** exhibited I_{DS}−V_G characteristics quite similar to those of **4**. OTFT devices using as-spun **5** films without thermal annealing showed a mobility of around 0.63 $cm^2 \cdot V^{-1} \cdot s^{-1}$ (Figure 4a), and after the sample was annealed at 180 °C, the mobility abruptly increased to 1.5 $cm^2 \cdot V^{-1} \cdot s^{-1}$ ($I_{on}/I_{off} \approx 10^6$, V_{th} = −12 V) (Figure 4b). Surprisingly, the maximum mobilities of the two polymers were determined to be higher than 1.0 $cm^2 \cdot V^{-1} \cdot s^{-1}$; however, the TFTs with **5** films showed a little higher mobility than the TFTs with **4** films. It was found that polymer **5** has a much smaller M_n than **4**, which can aid the solubilization of the selenophene-containing polymer. The strong interchain interaction in P(DPP-*alt*-DTBSe), **5**, induced slightly denser chain packing than in P(DPP-*alt*-QT), **4**, which is supported by the XRD results (see Figure 8S). The topography in the AFM images displayed highly developed crystalline fibrous structures in both the pristine and annealed **5** films, which is different from the images in the **4** films (Figures 9S and 10S). The selenophene-containing polymer with relatively low M_n showed obvious improvement in physical properties as well as the device properties. In brief, the significantly large mobilities are attributed to the strong tendency toward strong D−A interaction between the DPP acceptor unit and the alternating donor units in both polymers, which leads to closer alignment of the polymer, thereby facilitating charge transport in the film state.

In conclusion, we prepared novel conjugated alternating copolymer with DPP and DTBSe monomers, including a DPP-QT-based copolymer. This polymer, **5**, exhibited a significantly high hole mobility ($\mu \approx$ 1.5 $cm^2 \cdot V^{-1} \cdot s^{-1}$), higher than 1.0 $cm^2 \cdot V^{-1} \cdot s^{-1}$, which is one of the highest values obtained thus far from a homogeneous polymer system. Besides the π−π interactions between identical conjugative moieties, donor−acceptor dyad interactions were the most important driving force in the construction of a well-ordered morphological structure, which facilitates the charge transport phenomenon. In particular, **5** showed promising physical properties and device performances in terms of the carrier mobility and good solubility accompanied with great film-forming properties.

This study unambiguously demonstrates that the DPP and DTBSe alternating copolymer with a relatively low M_n, high degree of crystallinity, and great solubility can be effectively utilized for fabricating significantly improved OTFT devices.

■ ASSOCIATED CONTENT

Supporting Information. Complete experimental details of syntheses, ^{1}H NMR spectra, GPC chromatogams of polymers, and device fabrication; magnified images of optical micrographs and atomic force micrographs; output and transfer curves of TFT devices; and complete ref 9e. This material is available free of charge via the Internet at http://pubs.acs.org.

■ AUTHOR INFORMATION

Corresponding Author
dhchoi8803@korea.ac.kr

■ ACKNOWLEDGMENT

This research was supported by the National Research Foundation (NRF) of Korea (No. 20100025252) and by Priority Research Centers Program through the NRF funded by the Ministry of Education, Science and Technology (NRF2011-0018396).

■ REFERENCES

(1) Zhang, Y.; Petta, J. R.; Ambily, S.; Shen, Y.; Ralph, D. C.; Malliaras, G. G. *Adv. Mater.* **2003**, *15*, 1632.
(2) Klauk, H.; Halik, M.; Zschieschang, U.; Schmid, G.; Radlik, W. *J. Appl. Phys.* **2002**, *92*, 5259.
(3) Li, Z.; Du, J.; Tang, Q.; Wang, F.; Xu, J. B.; Yu, J. C.; Miao, Q. *Adv. Mater.* **2010**, *22*, 3242.
(4) Zhang, L.; Tan, L.; Wang, Z.; Hu, W.; Zhu, D. *Chem. Mater.* **2009**, *21*, 1993.
(5) Gao, P.; Beckmann, D.; Tsao, H. N.; Feng, X.; Enkelmann, V.; Baumgarten, M.; Pisula, W.; Müllen, K. *Adv. Mater.* **2009**, *21*, 213.
(6) McCulloch, I.; Heeney, M.; Bailey, C.; Genevicius, K.; MacDonald, I.; Shkunov, M.; Sparrowe, D.; Tierney, S.; Wagner, R.; Zhang, W.;

Chabinyc, M. L.; Kline, R. J.; McGehee, M. D.; Toney, M. F. *Nat. Mater.* **2006**, *5*, 328.
(7) Umeda, T.; Kumaki, D.; Tokito, S. *J. Appl. Phys.* **2009**, *105*, 024516.
(8) Nelson, T. L.; Young, T. M.; Liu, J.; Mishra, S. P.; Belot, M. J.; Balliet, C. L.; Javier, A. E.; Kowalewski, T.; McCullough, R. D. *Adv. Mater.* **2010**, *22*, 4617.
(9) (a) Tsao, H. N.; Cho, D.; Andreasen, J. W.; Rouhanipour, A.; Breiby, D. W.; Pisula, W.; Müllen, K. *Adv. Mater.* **2009**, *21*, 209. (b) Zhang, W.; Smith, J.; Watkins, S. E.; Gysel, R.; McGehee, M.; Salleo, A.; Kirkpatrick, J.; Ashraf, S.; Anthopoulos, T.; Heeney, M.; McCulloch, I. *J. Am. Chem. Soc.* **2010**, *132*, 11437. (c) Li, Y.; Singh, S. P.; Sonor, P. *Adv. Mater.* **2010**, *22*, 4862. (d) Li, Y.; Sonar, P.; Singh, S. P.; Soh, M. S.; van Meurs, M.; Tan, J. *J. Am. Chem. Soc.* **2011**, *133*, 2198. (e) Bronstein, H.; et al. *J. Am. Chem. Soc.* **2011**, *133*, 2198. (f) Tsao, H. N.; Cho, D. M.; Park, I.; Hansen, M. R.; Mavrinskiy, A.; Yoon, D. Y.; Graf, R.; Pisula, W.; Spiess, H. W.; Müllen, K. *J. Am. Chem. Soc.* **2011**, *133*, 2605.
(10) Hamilton, R.; Smith, J.; Ogier, S.; Heeney, M.; Anthony, J. E.; McCulloch, I.; Veres, J.; Bradley, D. C.; Anthopoulos, T. D. *Adv. Mater.* **2009**, *21*, 1166.
(11) Smith, J.; Heeney, M.; McCulloch, I.; Malik, J. N.; Stingelin, N.; Bradley, D. D. C.; Anthopoulos, T. D. *Org. Electron.* **2011**, *12*, 143.
(12) van Breemen, A. J. J. M.; Herwig, P. T.; Chlon, C. H. T.; Sweelssen, J.; Schoo, H. F. M.; Benito, E. M.; de Leeuw, D. M.; Tanase, C.; Wildeman, J.; Blom, P. W. M. *Adv. Funct. Mater.* **2005**, *15*, 872.
(13) Usta, H.; Lu, G.; Facchetti, A.; Marks, T. J. *J. Am. Chem. Soc.* **2006**, *128*, 9034.
(14) Ong, B. S.; Wu, Y.; Liu, P.; Gardner, S. *Adv. Mater.* **2005**, *17*, 1141.
(15) Heeney, M.; Bailey, C.; Genevicius, K.; Shkunov, M.; Sparrowe, D.; Tierney, S.; McCulloch, I. *J. Am. Chem. Soc.* **2005**, *127*, 1078.
(16) Fukuda, M.; Kodoma, K.; Yamamoto, H.; Mito, K. *Dyes Pigm.* **2004**, *63*, 115.
(17) Choi, S. H.; Kwon, O. T.; Kim, N. R.; Yoon, C.; Kim, J. P.; Choi, J. H. *Bull. Kor. Chem. Soc.* **2010**, *4*, 1073.
(18) Sonar, P.; Ng, G. M.; Lin, T. T.; Dodabalapur, A.; Chen, Z. K. *J. Mater. Chem.* **2010**, *20*, 3626.
(19) Guo, F.; Qu, S.; Wu, W.; Li, J.; Ying, W.; Hua, J. *Synth. Met.* **2010**, *160*, 1767.
(20) Beyerein, T.; Tieke, B. *Macromol. Rapid Commun.* **2000**, *21*, 182.
(21) Sonar, P.; Singh, S. P.; Li, Y.; Soh, M. S.; Dodabalapur, A. *Adv. Mater.* **2010**, *22*, 5409.
(22) Bijleveld, J. C.; Gevaerts, V. S.; Nuzzo, D. D.; Turbiez, M.; Mathijssen, S. G. J.; de Leeuw, D. M.; Wienk, M. M.; Janssen, R. A. *Adv. Mater.* **2010**, *22*, E242.
(23) Chen, Z.; Lekme, H.; Seifried, S. A.; Caironi, M.; Nielsen, M. M.; Heeney, M.; Zhang, W.; McCulloch, I.; Sirringhaus, H. *Adv. Mater.* **2010**, *22*, 2371.
(24) Kong, H.; Jung, Y. K.; Cho, N. S.; Kang, I. N.; Park, J. H.; Cho, S.; Shim, H. K. *Chem. Mater.* **2009**, *21*, 2660.
(25) Kong, H.; Chung, D. S.; Kang, I. N.; Park, J. W.; Park, M. J.; Jing, I. H.; Park, C. E.; Shim, H. K. *J. Mater. Chem.* **2009**, *19*, 3490.
(26) Fong, H. H.; Pozdin, V. A.; Amassian, A.; Malliaras, G. G.; Smilgies, D. M.; He, M.; Gasper, S.; Zhang, F.; Sorensen, D. M. *J. Am. Chem. Soc.* **2008**, *130*, 13202.
(27) Kim, Y. M.; Lim, E. H.; Kang, I. N.; Jung, J. B.; Lee, J. M.; Koo, B. W.; Do, L. M.; Shim, H. K. *Macromolecules* **2006**, *39*, 4081.
(28) Cao, D.; Liu, Q.; Zeng, W.; Han, S.; Peng, J.; Liu, S. *J. Polym. Sci. Part A: Polym. Chem.* **2006**, *44*, 2395.
(29) Kanimozhi, C.; Balraju, P.; Sharma, G. D.; Patil, S. *J. Phys. Chem. B* **2010**, *114*, 3095.
(30) Qiao, Z.; Peng, J.; Jin, Y.; Liu, Q.; Weng, J.; He, Z.; Han, S.; Cao, D. *Polymer* **2010**, *51*, 1016.